

Behavior of UHPC Column Subjected to Combined Axial and Lateral Loading

Author(s) & Affiliation:

Mahmoud Aboukifa – PhD Student, Civil and Environmental Engineering, University of Nevada, Reno, NV 89557 USA, Email: maboukifa@nevada.unr.edu

Mohamed Moustafa, Ph.D., P.E.,* (corresponding author) – Assistant Professor, Civil and Environmental Engineering, University of Nevada, Reno, NV 89557 USA, Phone: 775-682-7919, Email: mmoustafa@unr.edu

Ahmad Itani, Ph.D., P.E., S.E. – Professor and Chair, Civil and Environmental Engineering, University of Nevada, Reno, NV 89557 USA, Phone: 775-682-7919, Email: itani@unr.edu

Abstract:

Ultra-High Performance Concrete (UHPC) is a versatile building material as it is characterized by very high compressive strengths reaching 200 MPa (30 ksi), ductile tensile characteristics, and energy absorption. Currently, UHPC is commonly used in small structural applications, such as joints and connections between precast structural elements. However, this material is not widely used in structural elements due to the lack of knowledge of the structural behavior and failure mechanism of these elements. There is a great potential for application of UHPC in full structural elements, e.g. highly stressed compression members of high rise buildings, industrial buildings, bridge columns, and members with high durability requirements in aggressive environmental conditions. This study investigated the behavior of UHPC columns subjected to combined axial and lateral loading. A large-scale UHPC column is tested under axial and quasi-static cyclic lateral loading at the Earthquake Engineering Laboratory at the University of Nevada, Reno. The lateral response of these columns is evaluated for damage progression, failure type, peak strength, and displacement and curvature ductility.

Keywords: Columns; large-scale testing; seismic behavior; ductility.

1. Introduction

Over the past few decades, ultra-high performance concrete (UHPC) has advanced notably in the structural applications, specifically, in highway and pedestrian bridges. The development of UHPC to have high compressive strengths reaching 200 Mpa (30 Ksi), it is now possible to widen its applications to build highly loaded columns with reduced cross sections to meet the demands of high rise buildings and bridge piers. Many studies have been conducted on the UHPC at the material level to investigate the material's properties. The results of these studies showed that UHPC have many advantages over the conventional concrete, including high compressive strength (Graybeal 2007), high tensile strength and post-cracking tensile ductility (Graybeal and Baby 2013), a very high durability (Graybeal and Tanesi 2007), and low shrinkage and creep (Burkart and Mullar 2008; Graybeal 2006). Other studies considered UHPC at the structural level with main focus on the accelerated bridge construction applications, e.g. bonding of the UHPC to steel reinforcement (Marchand et al. 2016; Saleem et al. 2013; Yuan and Graybeal 2015), the

connections between the prefabricated-bridge-deck slabs (El-Tawil et al. 2016; Graybeal 2010; Verger-Leboeuf et al. 2017), and UHPC-filled ducts for precast column-to-footing connection (Tazarv and Saiidi 2014).

In the past few years, efforts have been made to widen the use of UHPC in columns to make use of its outstanding compressive strength and high ductility. An experimental study was made on UHPC columns under pure axial loading (Hosinieh et al. 2015). It was concluded that for a particular transverse reinforcement configuration, using of cross ties, and reduction of the confinement steel results in enhancement of columns post-peak ductility with a moderate increase in the column capacity under axial loads. A preliminary analytical study was conducted by Joe and Moustafa (2016) to investigate the design implications of using UHPC for seismic bridge columns in lieu of conventional concrete. They showed that up to 40% reduction in the columns cross-section can be obtained if UHPC is used to achieve same plastic moment capacity and ductility compared to the use of conventional concrete. An experimental study by Chao et al. (2016) investigated the seismic response of UHPC beams and columns with relatively higher amounts of longitudinal reinforcement ($>2.5\%$). Based on their research, UHPC columns have higher strength and drift capacity before significant strength degradation, compared to RC columns. The concrete spalling and crushing, bar buckling and hoop failure are significantly reduced in UHPC columns. The researchers also showed that the confinement requirements and amount of transverse reinforcement can be reduced for high strength concrete (>10 ksi) columns. Another study was made by Hung and Hu (2018) to experimentally investigate the behavior of ten slender high-strength concrete of 100 MPa compressive strength and steel fiber contents ranging from 0% to 1.5% under concentric axial loads. They found that inclusion of 1.5% fibers enhanced the post-peak behavior as it became more ductile and it controlled the cover spalling preventing the longitudinal rebars from buckling.

In summary, small-scale UHPC columns were investigated under pure axial loading, however limited research was performed on large-scale UHPC columns under combined axial and lateral loading. In this paper, a large scale UHPC column has been subjected to both axial compression and alternate transverse loading, resulting in an alternate bending moment. The main focus is to investigate the seismic response of the UHPC column with respect to damage progression, failure type, peak strength, displacement and curvature ductility.

2. Experimental Program

The experimental program presented herein is a part of an ongoing larger and more comprehensive study consisting of four large scale columns with different longitudinal reinforcement grade and ratio, and different confinement ratio. However, only the results from the UHPC column with grade 60 longitudinal rebars and code-compliant lateral reinforcement is presented here.

2.1 Specimen Design and Construction

The specimen as shown in Figure 1 was designed to represent a 1/5 scale of a typical normal strength concrete (NSC) California bridge column. The height and diameter of the UHPC column were 1.47 m (58 in.) and 254 mm (10 in.), respectively. The UHPC column was reinforced longitudinally with 6 #5 ($\Phi 16$ -mm) bars and transversely with a #3 at 2 in. spacing ($\Phi 10$ -mm at 51 mm spacing), resulting in longitudinal and transverse steel ratios of 2.37% and 1.1%, respectively. The footing was designed to be capacity protected and consisted of two parts: an UHPC inner part connected to the UHPC column to ensure the continuity in the plastic hinge

region, and NSC footing. The plan dimensions were $0.6 \times 0.6 \text{ m}^2$ ($2 \times 2 \text{ ft}^2$) for UHPC part and external dimensions of $1.52 \times 1.52 \text{ m}^2$ ($5 \times 5 \text{ ft}^2$) for NSC and both parts were 355 mm (14 in.) deep.

The construction stages of the specimen consisted of the following: (1) casting the NSC outer part of the footing (Figure 2a); (2) casting the UHPC inner part of the footing (Figure 2b); (3) casting of the UHPC column (Figure 2c) along with an UHPC column head (Figure 2d). It is noted that the joint type between each two consecutive casting stages was a cold joint which means that each casting stage was done after the previous cast get hardened.

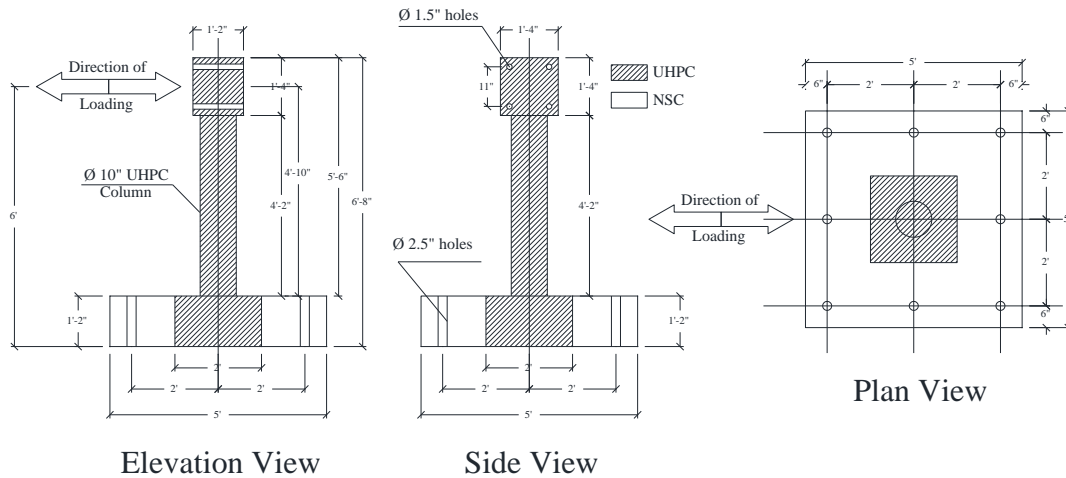


Figure 1. Specimen Dimensions



Figure 2. Specimen Construction Stages: (a) Casting of NSC Footing; (b) Casting of UHPC Footing; (c) Casting of UHPC Column; (d) Casting of UHPC Column Head.

2.2 Material Properties

Cylinders of UHPC of $76.2 \times 152.4 \text{ mm}$ ($3 \times 6 \text{ in}$) dimensions were tested at 14 days and at the column test day (64 days). A summary of the measured compressive strength of the materials is presented in Table 1. The reported material strengths are the average of a minimum of three cylinders tested for every material at each stage of construction. The UHPC cylinders were surface prepared using a grinding machine to get smooth flat surfaces for accurate strength evaluation. The longitudinal steel reinforcement used was ASTM A706 Grade 60 (ASTM 2009). The measured yield and ultimate tensile strength of the longitudinal reinforcing steel bars were 485.6 MPa (70.4

ksi) and 697.8 MPa (101.2 ksi), respectively. The yielding strain was 0.23% and the ultimate elongation is 19%.

Table 1. Measured Compressive Strength of specimen's members

Material	Element	Measured at	Strength, MPa (ksi)
UHPC	Inner Footing	14 days	173.6 (25.18)
		Test day	216.4 (31.38)
	Column	14 days	169.7 (24.62)
		Test day	204.4 (29.64)
	Column head	14 days	176.6 (25.62)
		Test day	208 (30.17)

2.3 Test Setup and Loading Protocol

The column was tested in a cantilever configuration setup as shown in Figure 3. The axial load index, which is the ratio of the axial load to the product of column gross section area and the specified compressive strength of the concrete column, was kept constant at 5% during the test. The axial load was applied to the top of the column through two center-hole rams placed on a load spreader beam perpendicular to the lateral load direction to apply approximately 534 kN (120 kip) axial load to the column. The cyclic loading was applied through a servo-hydraulic actuator with displacement-controlled loading. The selected loading protocol was adopted from FEMA 461 (FEMA 2007) where every applied cycle is a ratio of the column displacement at which the longitudinal reinforcing bars yield as shown in Figure 4. The loading also applied two full cycles for each drift ratio, and after reaching the yield displacement, a small cycle with half the yield displacement was applied after each two complete main cycles to capture the stiffness degradation with increasing the drift ratio. Two displacement rates of 0.25 mm/sec (0.01 in./sec) and 1.27 mm/sec (0.05 in./sec) were used with the former used for drift ratios up to 3% and the latter used for larger drift ratios.

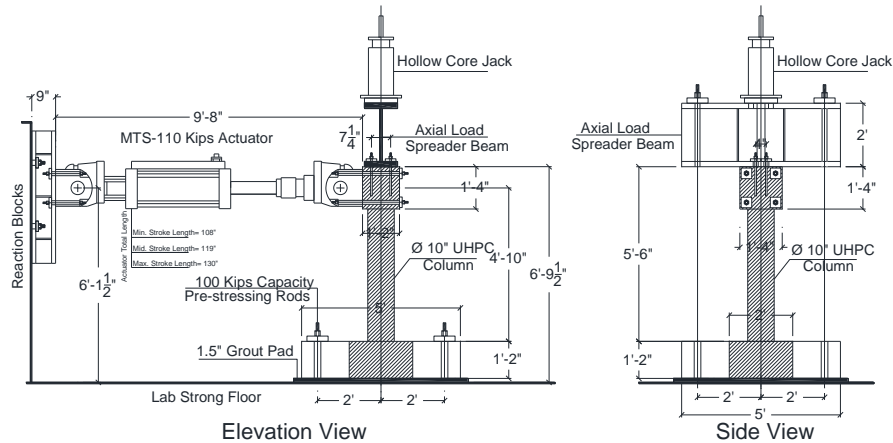


Figure 3. Test Setup for UHPC column under combined axial and bending

2.4 Instrumentation Plan

As shown in Figure 5, the specimen was instrumented with 21 reinforcement strain gages to capture the longitudinal and transverse bars strains in the column plastic hinge region. Three string pots were attached to the column head to capture the column top displacement. Ten

displacement Transducers were attached to the column plastic hinge region as shown in Figure 5 to capture the column curvature at the different drift ratios.

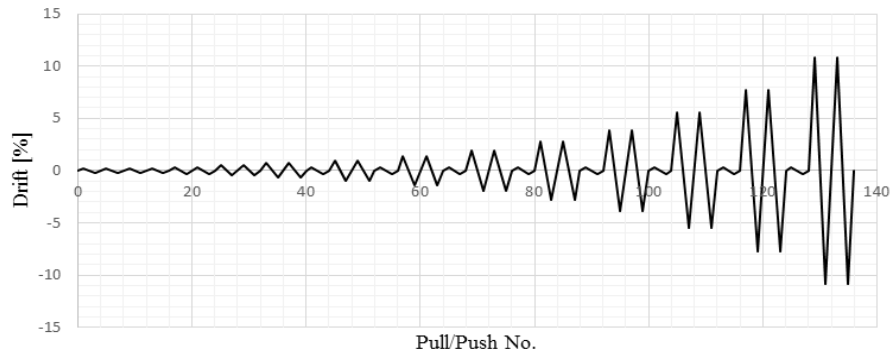


Figure 4. Cyclic Loading Protocol

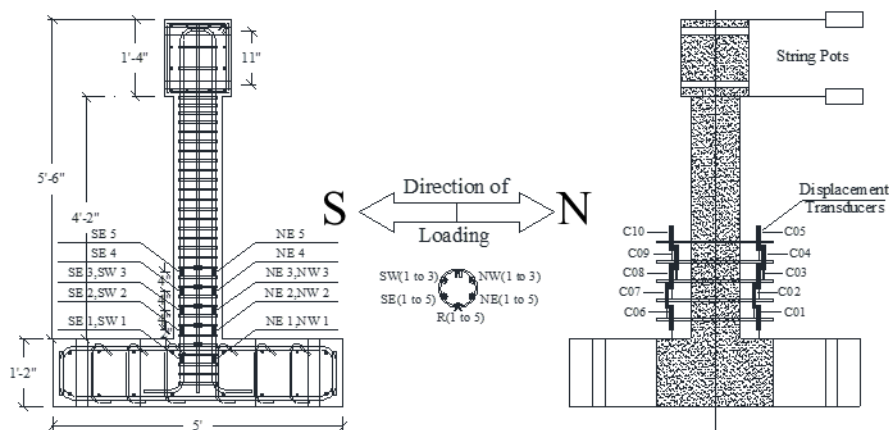


Figure 5. Specimen instrumentation types and layout

3. Test Results and Discussion

In this section, the column test results are discussed from a global and local behavior perspectives.

3.1 Column Global Behavior

3.1.1 Plastic Hinge Damage and Mode of Failure

The observed mode of failure for the UHPC column was the fracture of reinforcing bars. The test was stopped after the rupture of the four outer-most rebars in the north and south directions of the column and before the rupture of the two middle rebars for test setup stability purposes. The first bar ruptured at the second cycle of almost 8% drift ratio while the other three bars ruptured at almost 11% drift ratio cycles. There was no evidence of rebar buckling. Furthermore, no concrete spalling or reinforcement exposure was observed until the end of the test. No cracks were observed until reaching 1% drift ratio. The onset of UHPC crushing in compression was observed at 2.76% drift ratio and the first significant crack started to appear at level 5.08 cm (2 in) above the footing at 4% drift ratio with 0.76 mm (0.03 in) crack width. A wide crack appeared at the column-footing interface at drift ratio 8% with almost 2.54 mm (0.1 in) crack width. Figure 6a shows the plastic hinge damage of the column at 10.83% drift ratio. Moreover, the stiffness degradation of the UHPC column was investigated. It was observed that the column lost 50% of its initial stiffness after

reaching 2% drift ratio. It is also noted that the column initial stiffness was 7.35 kN/mm (42 kips/in.), almost equal to $0.7E_cI_g$ based on the UHPC modulus of elasticity recommended by Graybeal (2007).

3.1.2 Force-Displacement Relationship

Figure 6b shows the hysteretic behavior of the UHPC column along with the backbone envelope. The positive values on the plot indicate pushing the column towards north direction. The asymmetric response is due to a distorted pattern locations of the six longitudinal rebars that occurred during construction. The peak strength was reached and maintained at drift ratios 5.5% and 7.7% for the pull and push directions, respectively. The first bar yielding and rupture were observed at drift ratios of 0.92% and 7.7%, respectively. The measured displacement ductility was almost 8.4 which meets and exceed the AASHTO (2014) requirements for maximum displacement ductility demand of 5. It is also seen from Figure 6b that the column has more than 65% reserved displacement capacity, which allows UHPC columns to be used in high seismic regions.

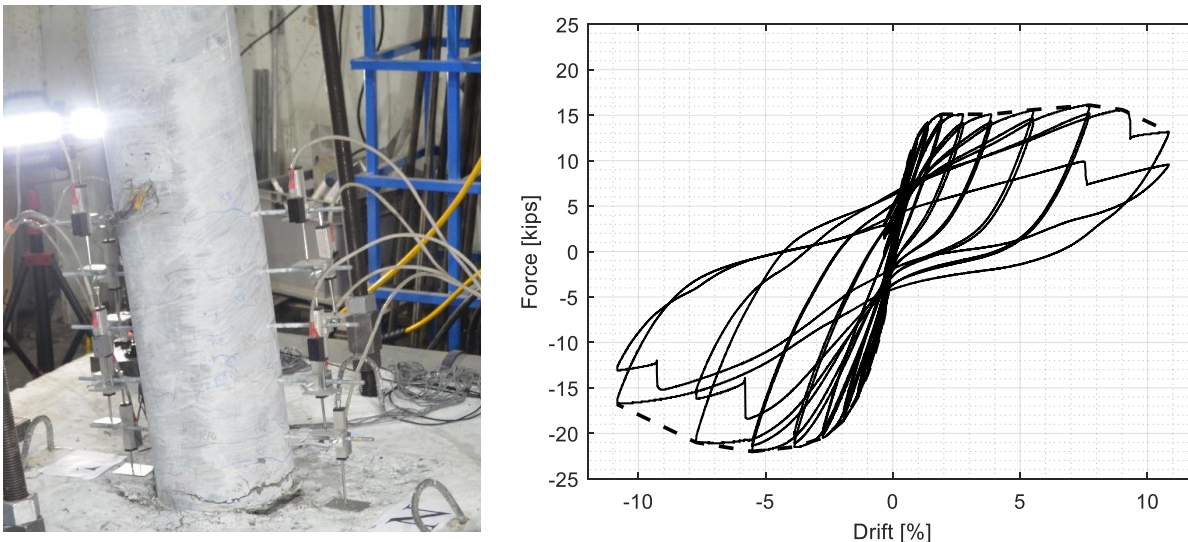


Figure 6. Plastic hinge damage at 10.83% drift ratio (left); global force-drift relationship (right)

3.2 Column Local Behavior

3.2.1 Strains

The longitudinal reinforcement strain profiles at the plastic hinge region are shown in Figure 7. The strains values reported in the figure are the maximum absolute strains of the two complete cycles at each drift ratio. A sample of the strain gage profiles is reported and shown at 0.97, 1.93 and 3.86% drift ratios. It can be seen that the reinforcing bar strains were well distributed in the plastic hinge region of the column-footing interface.

3.2.2 Curvature Profiles and Moment-Curvature Behavior

The curvature profiles at the plastic hinge region reported at different drift levels are shown in Figure 8. Curvatures were measured indirectly by using displacement transducers mounted on both loading sides of the columns as illustrated before in Figure 5. Curvatures at each level were computed as the ratio of the section rotations of that level to the vertical distance of the transducers,

where in turn, the rotations were the ratio of the summation of the relative displacements to the horizontal distance between the transducers in the same level. The moment curvature relationship was also obtained and shown in Figure 9. The maximum moment capacities in the push and pull loading sides are 105.4 (933 kip-in) and 144.2 kN.m (1,276 kip.in), respectively. The curvature ductility is determined to be equal to 15.4, which is comparable to typical ductile NSC columns.

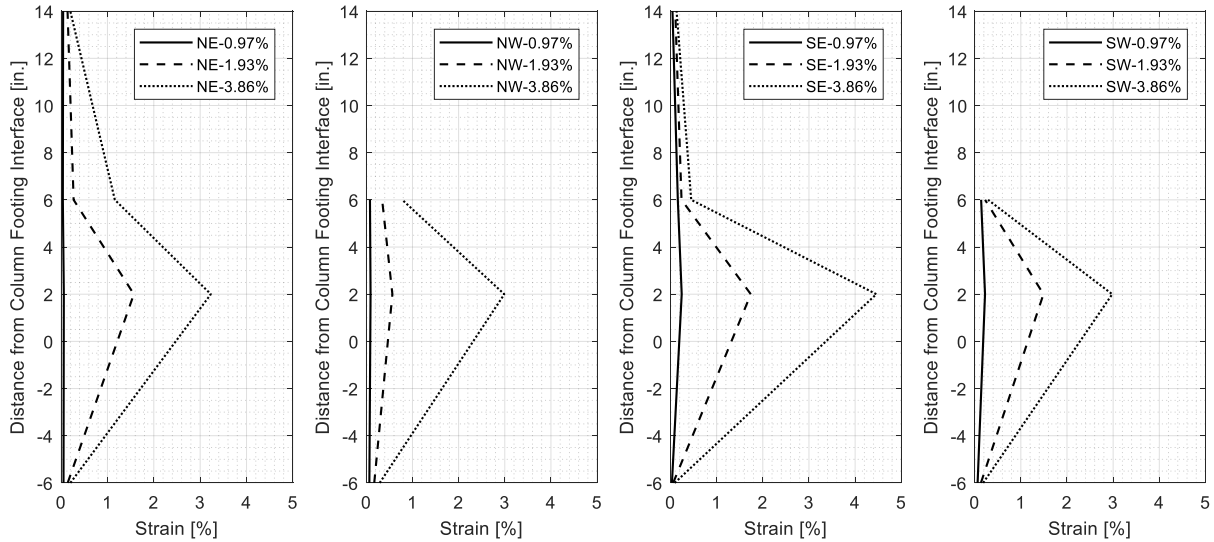


Figure 7. Distribution of the longitudinal rebars strains within plastic hinge region

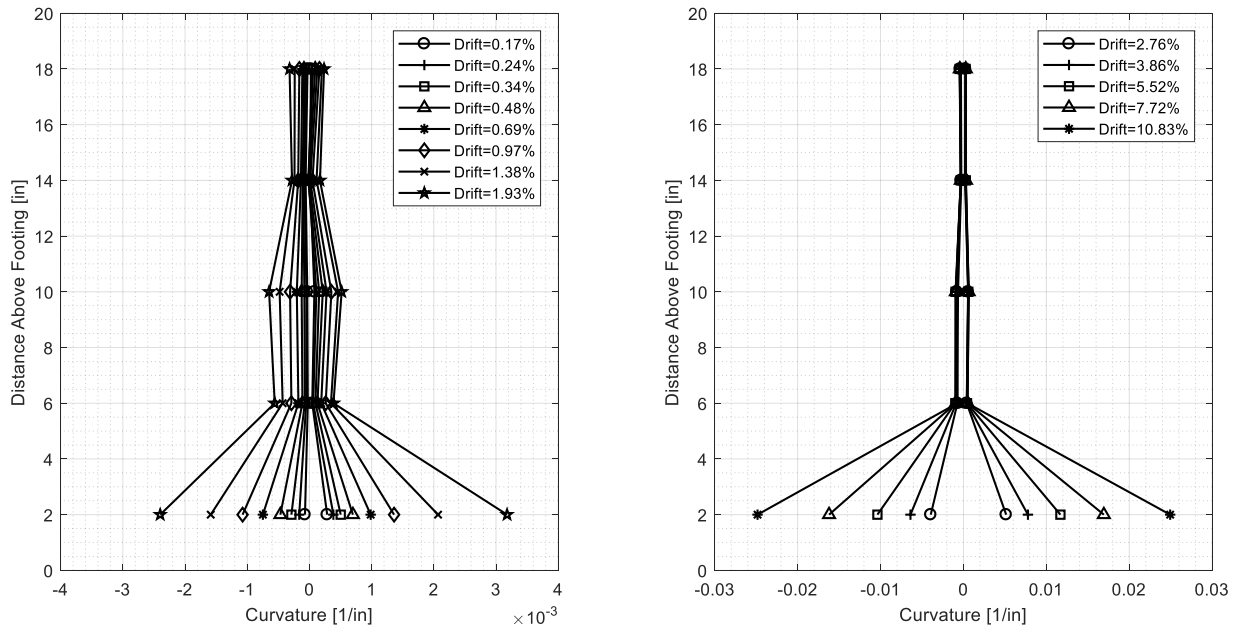


Figure 8. Distribution of the UHPC column curvatures within plastic hinge region

4. Concluding Remarks

This study presents the structural and seismic response of an UHPC column under combined axial and cyclic loading. Overall, the UHPC column featured a ductile behavior with adequate moment capacity. Few observations and concluding remarks are as follows:

- The observed mode of failure for the UHPC column was tensile rupture of the longitudinal rebars without any concrete spalling.
- The first longitudinal rebar yield was observed at 0.92% drift, while the onset of UHPC concrete crushing in the compression side was observed at 2.76% drift ratio.
- The UHPC column showed an adequate ductile behavior that is with the displacement and curvature ductility found to be 8.4 and 15.4, respectively.
- The initial column flexural stiffness measured at 0.17% drift was equivalent to 0.7 times the product of Young's modulus and gross moment of inertia, then dropped to almost 50% at 2% drift.

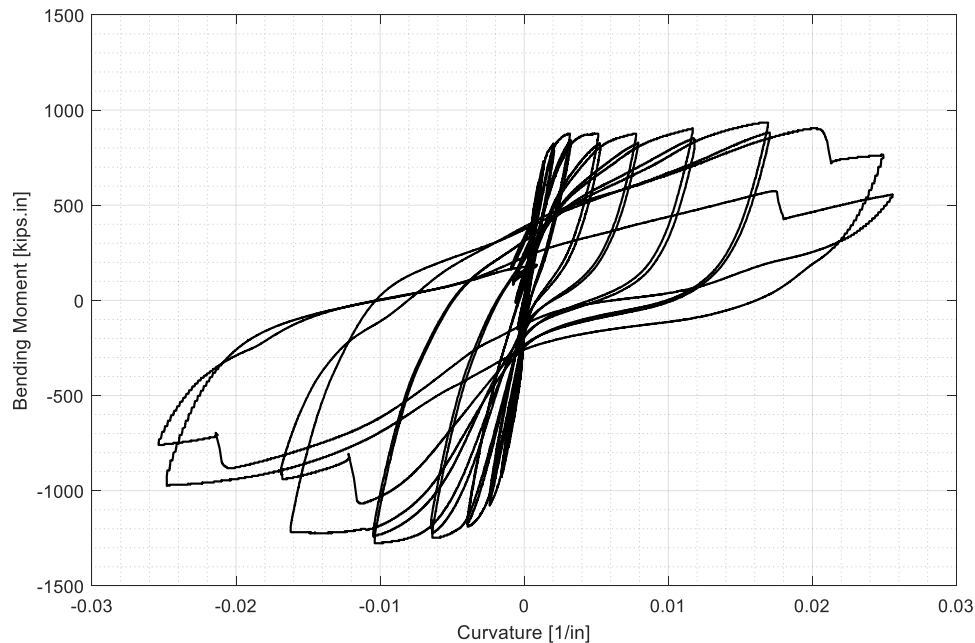


Figure 9. Bending Moment-Curvature Hysteretic Curve

5. References

- AASHTO. (2014). AASHTO guide specifications for LRFD seismic bridge design, Washington, DC.
- ASTM. (2009). "Standard specification for low-alloy steel deformed and plain bars for concrete reinforcement." A706/A706M-09b, West Conshohocken, PA.
- Burkart, I., & Müller, H. S. (2008, March). Creep and shrinkage characteristics of ultra high strength concrete (UHPC). In Proceedings of the Second International Symposium on Ultra High Performance Concrete (pp. 469-476).
- Chao, Shih-Ho & Venkatesh, Kaka & Palacios, Guillermo & Kim, Jinsup & Choi, Youngjae & Aghdasi, Parham & Nojavan, Alireze & Schultz, Arturo. (2016). Seismic Behavior of Ultra-High-Performance Fiber-Reinforced Concrete Moment Frame Members. 10.21838/uhpc.2016.44.
- El-Tawil, S., Alkaysi, M., Naaman, A. E., Hansen, W., & Liu, Z. (2016). Development, characterization and applications of a non proprietary ultra high performance concrete for highway bridges (No. RC-1637). Department of Civil and Environmental Engineering, University of Michigan.

- Federal Emergency Management Agency (FEMA). (2007). FEMA 461: Interim Testing Protocols for Determining the Seismic Performance Characteristics of Structural and Nonstructural Components.
- Graybeal, B. A. (2006). Material property characterization of ultra-high performance concrete (No. FHWA-HRT-06-103).
- Graybeal, B. A. (2007). Compressive behavior of ultra-high-performance fiber-reinforced concrete. *ACI materials journal*, 104(2), 146.
- Graybeal, B. A. (2010). Behavior of field-cast ultra-high performance concrete bridge deck connections under cyclic and static structural loading (No. FHWA-HRT-11-023). United States. Federal Highway Administration.
- Graybeal, B. A., & Baby, F. (2013). Development of Direct Tension Test Method for Ultra-High-Performance Fiber-Reinforced Concrete. *ACI Materials Journal*, 110(2).
- Graybeal, B., & Tanesi, J. (2007). Durability of an ultrahigh-performance concrete. *Journal of materials in civil engineering*, 19(10), 848-854.
- Hosinieh, M. M., Aoude, H., Cook, W. D., & Mitchell, D. (2015). Behavior of ultra-high performance fiber reinforced concrete columns under pure axial loading. *Engineering Structures*, 99, 388-401.
- Hung, C. C., & Hu, F. Y. (2018). Behavior of high-strength concrete slender columns strengthened with steel fibers under concentric axial loading. *Construction and Building Materials*, 175, 422-433.
- Joe, C. D., & Moustafa, M. A. (2016). Cost and Ecological Feasibility of Using UHPC in Bridge Piers. In *First International Interactive Symposium on UHPC* (pp. 18-20).
- Marchand, P., Baby, F., Khadour, A., Battesti, T., Rivillon, P., Quiertant, M., ... & Toutlemonde, F. (2016). Bond behaviour of reinforcing bars in UHPFRC. *Materials and structures*, 49(5), 1979-1995.
- Saleem, M. A., Mirmiran, A., Xia, J., & Mackie, K. (2012). Development length of high-strength steel rebar in ultrahigh performance concrete. *Journal of Materials in Civil Engineering*, 25(8), 991-998.
- Tazarv, M., and M. Saiid Saiidi. 2014. Next generation of bridge columns for accelerated bridge construction in high seismic zones. Technical Rep. No. CA14-2176. Reno, NV: Univ. of Nevada.
- Verger-Leboeuf, S., Charron, J. P., & Massicotte, B. (2017). Design and Behavior of UHPFRC Field-Cast Transverse Connections between Precast Bridge Deck Elements. *Journal of Bridge Engineering*, 22(7), 04017031.
- Yuan, J., & Graybeal, B. (2015). Bond of Reinforcement in Ultra-High-Performance Concrete. *ACI Structural Journal*, 112(6).